Journal of Electroceramics, 7, 25–34, 2001

Crystal and Defect Chemistry of Rare Earth Cations in $BaTiO_3$

YOED TSUR,[1,*] TIMOTHY D. DUNBAR[2] & CLIVE A. RANDALL[1]

[1] *Center for Dielectric Studies, Materials Research Laboratory, The Pennsylvania State University, University Park, PA 16802-4800, USA*
[2] *Sandia National Labs, PO Box 5800; MS 1405, Albuquerque, NM 87186-1405, USA*

Submitted September 20, 2000; Revised June 4, 2001; Accepted June 11, 2001

Abstract. This study revisits the issue of rare earth cation substitutions into barium titanate. Analysis based upon crystal chemistry, defect chemistry and metastable states is presented to aid interpretation of experimental data. Recent detailed and highly precise X-ray powder diffraction and Electron Paramagnetic Resonance experiments performed on samples produced with different A/B ratios and fired under different oxygen partial pressure conditions give rise to new insights into the material. Specifically, the site occupancy and the valence states for the rare-earth dopants in barium titanate are considered. Earlier work is also reviewed and compared to the studies performed here. Collectively a classification of the various types of behavior observed for the rare-earth series in barium titanate is presented.

Keywords: amphoteric, multilayer capacitors, site occupancy, base metal dielectrics, perovskites, point defects

1. Introduction

Many cation dopants are highly soluble in $BaTiO_3$, and are used to engineer the electrical properties of the material. The $BaTiO_3$ material is used for a number of electro-optic, electromechanical and dielectric applications, but the largest commercial markets are positive temperature coefficient resistors (PTCR) and multilayer capacitors (MLC) [1]. Both PTCR and MLC $BaTiO_3$ materials often have formulation involving the incorporation of rare-earth cations to control conductivity and electrical degradation, respectively [2, 3]. It is the latter of these two applications that pulled this investigation. In particular, dopants such as Ho and Dy which give rise to amphoteric behavior (A- or B-site occupancy) and maximize the lifetime of base metal multilayer capacitors.

The objective of this study is to give a detailed account of the various types of behavior that can be observed in doping $BaTiO_3$ with rare-earths and classify the various phenomena observed. The trends are discussed in terms of the defect and crystal chemistry of the host $BaTiO_3$ crystal. The rare-earths are first considered as a series of 3+ cations with gradual change in their ionic radii. Second, other valences are also considered with relation to the temperature, oxygen partial pressure and site occupancy. Earlier experimental works are reviewed as well as our own XRD and EPR measurements. Finally, a summary is given in the form of a short note for each of the rare-earth dopants, except the radioactive Pm.

*Current address: Chemical Engineering Department, Technion—Israel Institute of Technology, Haifa 32000, Israel; E-mail: tsur@tx.technion.ac.il

2. Theoretical Considerations of Site Occupancy

2.1. Tolerance Factor Considerations

In an ideal cubic perovskite, the ionic radii, r_i $(i = A,\ B,\ O)$, satisfy the relation: $r_A + r_O = \sqrt{2}(r_B + r_O)$. The Goldschmidt tolerance factor for perovskites is, hence, defined by [4, 5]

$$t = \frac{r_A + r_O}{\sqrt{2}(r_B + r_O)} \tag{1}$$

For pure barium titanate, $t \simeq 1.06$. t is greater than 1 due to the fact that the Ti^{4+} ion is smaller than its cavity ($BaZrO_3$ has $t \simeq 1$) and/or that the Ba^{2+} is larger

than its cavity ($SrTiO_3$ has $t \simeq 1$). The substitutional chemistry cannot be determined by the tolerance factor alone. One should rather consider the tensoric nature of the strain, as well as charge and charge-distribution effects. However, for comparison of similar ions on the same site, the tolerance factor is a very useful tool that can give the correct trends. In addition, less reliable comparisons between different sites and different charge states can be made, provided the correct coordination numbers are considered, namely, 12 and 6 for the A- and B-sites respectively. For such comparisons, we define t_A and t_B as the tolerance factors for substitutional ions on the A- and B-sites respectively, taking into account the correct coordination number.

The tolerance factors t_A and t_B for the rare-earths 3+ ions R^{3+} are presented in Fig. 1 as functions of the ionic radius $r(R^{3+}_{\mathrm{VI}})$ where the subscript represents the coordination number. The ionic radii are taken from CRC [6] $r_O = r(\mathrm{O}^{2-}_{\mathrm{VI}}) = 1.40$ Å, $r(\mathrm{Ti}^{4+}_{\mathrm{VI}}) = 0.61$ Å and $r(\mathrm{Ba}^{2+}_{\mathrm{XII}}) = 1.61$ Å. Assuming that the local strain is similar in both sites, it is expected that if the incorporation into one site results in a tolerance factor much closer to unity than the incorporation into the other site, then the first one would be preferred over the second. It is therefore expected from the tolerance factors, see Fig. 1, that small ions ($r(R^{3+}_{\mathrm{VI}}) \lesssim 0.87$) will occupy the B-site, large ions ($r(R^{3+}_{\mathrm{VI}}) \gtrsim 0.94$) will occupy the A-site, and intermediate ions will occupy both sites with different partitioning for each ion. This will only hold for ions that are 3+ during the formation of the $BaTiO_3$ phase or grain growth; this we refer to as the incorporation process (see below). We note again that a comparison between ions in different sites based on tolerance factors, is only a qualitative one. Hence from this part one should expect a gradual change with the ionic radius from B-site to A-site occupancy, but the exact change-over point cannot be safely deduced. Yet, as we shall show later, there is a remarkable match between Fig. 1 (change-over at $r(R^{3+}_{\mathrm{VI}}) \approx 0.9$) and other quantitative techniques.

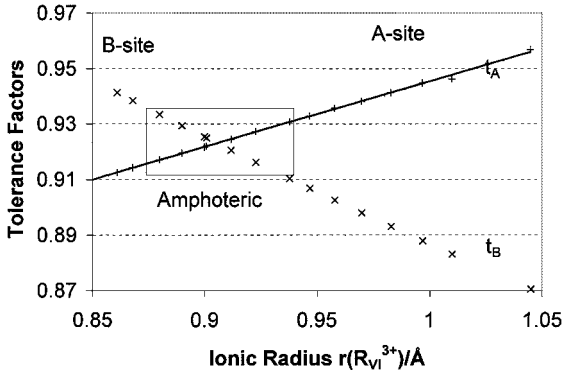

Fig. 1. The tolerance factors t_A and t_B for substitution of trivalent ions on the A- and B-sites, as functions of the ionic radius.

2.2. *Thermodynamic Considerations*

To gain understanding on what influences the site occupancy ratio, we consider the following two alternative incorporation reactions:

$$2\mathrm{Ti}^{x}_{\mathrm{Ti}} + \mathrm{O}^{\times}_{O} + R_2\mathrm{O}_3 \Rightarrow 2R'_{\mathrm{Ti}} + V^{\bullet\bullet}_{\mathrm{O}} + 2\mathrm{TiO}_2 \quad (2)$$

$$2\mathrm{Ba}^{x}_{\mathrm{Ba}} + V^{\bullet\bullet}_{\mathrm{O}} + 2\mathrm{TiO}_2 + R_2\mathrm{O}_3 \Rightarrow 2R^{\bullet}_{\mathrm{Ba}} + \mathrm{O}^{\times}_{O} + 2\mathrm{BaTiO}_3 \quad (3)$$

We use the Kröger–Vink notation [7] for point defects. Combining the corresponding mass action relations gives:

$$\frac{[R^{\bullet}_{\mathrm{Ba}}]}{[R'_{\mathrm{Ti}}]} = K(R,T)[V^{\bullet\bullet}_{\mathrm{O}}]\, a^2(\mathrm{TiO}_2) \quad (4)$$

where a is activity and R represents a given R^{3+} ion. Equations (2)–(4) hold only at very high temperatures, where all these species are mobile on a reasonable time scale [8]. As a rule of thumb, Eq. (4) is valid at temperatures whereby grain growth occur. We have previously used an alternative (and formally equivalent) presentation that links the site occupancy ratio to metal vacancy concentrations [9]

$$\frac{[R^{\bullet}_{\mathrm{Ba}}]}{[R'_{\mathrm{Ti}}]} \propto \frac{[V''_{\mathrm{Ba}}]}{[V''''_{\mathrm{Ti}}]} \quad (5)$$

This presentation assumes that the metal vacancy concentrations are not negligible. Since the latter assumption is under debate, we shall use here Eq. (4).

From Eq. (4) it follows that Ba-rich chemistry drives the ratio towards B-site and vice versa. However, one has to remember that this is only a ratio, i.e., the site occupancy ratio can still be very close to zero or very large for a particular impurity R. Since the charge difference of trivalent ion is ± 1 for both sites, it is expected that the ionic radius will influence the magnitude of K, as discussed above with relation to the

tolerance factors. Large ions will occupy the A-site (large K) and small ions will occupy the B-site (K approaches zero). The influence of the stoichiometry is most significant in the intermediate cases. In addition, the site occupancy ratio is $P(O_2)$ dependent. For simple cases it is proportional to the oxygen vacancy concentration, as shown theoretically and verified experimentally elsewhere [9] (see also Table 2 below). The simple proportionality can be also inferred from Eq. (4) for the particular case where the activity of titania is kept constant (namely, where there are two solid phases in equilibrium).

2.3. Kinetic Considerations

The cation sublattice can be easily frozen-in [8, 10]. Oxygen vacancies can migrate under electrochemical potential gradients relatively easily. This is because each oxygen vacancy has eight oxygen second-nearest neighbors into which it can hop. In the cation sublattice, however, the situation is quite different. A metal vacancy has eight second-nearest neighbors of the other metal site, and six third-nearest neighbors (and twelve fifth-nearest neighbors) of the same metal site. Hopping to the other metal site involves antisites, which are extremely unlikely due to size mismatch (for instance, Ba_{VI}^{2+} on the B-site gives tolerance factor of $t_B = 0.774$) and charge mismatch. Hopping between like metal sites is inhibited by the large potential barriers. However it is possible, but only at very high temperature and/or at surfaces. Impurities on the cation sublattice need metal vacancies in its neighbor in order to migrate. Therefore their migration also depends on the metal vacancy concentrations. The metal vacancy concentrations are believed to be higher near the surface [11]. It is therefore expected that impurities will migrate towards the surface during grain growth, until they are trapped in the bulk. The question of whether or not a core-shell structure with almost pure cores and highly doped shell barium titanate will be formed, is largely depends on the processing.

Of particular interest are rare-earth ions which are 3+ during the incorporation, and have comparable tolerance factors on both sites. These ions can migrate by hopping from one metal site into a neighboring vacancy on the other metal site. This makes the mobility of these ions larger than the mobility of other impurities, especially in space charge (high metal vacancy concentrations) regions.

To summarize this section, one expects equilibrium situations only at very high temperatures and in small grains. All other situations are metastable states. The most common metastable state can be described as a situation where the metal sublattice is practically frozen in, and the oxygen sublattice is in equilibrium with the surrounding. At lower (around room) temperature the oxygen sublattice is also practically frozen, as discussed by Sasaki and Maier [12]. Incorporation of impurities is by definition not a metastable state. However, impurities are expected to be frozen even at higher temperatures than the metal vacancies. Therefore the site occupancy is determined by the conditions at the initial incorporation and can not be easily changed by later treatments.

3. The Valence of the Dopant

The valence of the rare earth dopants is influenced by the surroundings. While most of the rare earths are rather stable as 3+ ions, some of them can assume either 2+ or 4+ valence states as well. For the less stable ions, the following parameters are to be considered:

- The site: A-site drives the rare-earth ion towards lower valence, while B-site drives it towards higher valence. This is due to both coulombic and strain energy contributions.
- Thermal energy: Higher temperature drives the ions towards higher valence.
- Electron/hole concentration (and oxygen partial pressure): For a given temperature, higher oxygen partial pressure give rise to higher concentration of holes and lower concentration of electrons. This drives the ions towards higher valence.

As explained in the previous section, the impurities choose their sites according to the local conditions during the incorporation. These impurities would not be expected to change their site at low temperatures. However, changes in valence depending on temperature and oxygen partial pressure may occur while the cation sublattice is in a metastable state.

4. Survey of Earlier Experimental Works

Investigations of site occupancy and properties of aliovalent doped $BaTiO_3$ were considered in several contexts and by different probes over the last 40 years [13–26]. In this section, some of the important experimental works are reviewed.

Rimai and deMars [13] reported using EPR that Gd^{3+} occupies the A-site in single crystal $BaTiO_3$. On the other hand, Takeda and Watanabe [14] reported using the same technique, that by increasing the Ba/Ti ratio some of the Gd^{3+} is found on the B-site, both in ceramic and single crystal samples. As far as we are aware, this was the first report on amphoteric behavior of trivalent ions in $BaTiO_3$. (Since site change of a well defined valence dopant cause change of the relative charge, we call these dopants amphoteric). Goodman [15] assumed that Sm occupies the A-site in Ti-rich single crystals and verified this assumption using Debye–Scherer XRD.

Rotenberg et al. [16] have shown that Lu^{3+} occupies the B-site, Sm^{3+} occupies the A-site and Er^{3+} is amphoteric. These researchers used a combination of experimental techniques, measuring the room temperature electrical resistivity [17] the cell volume and the Curie temperature as functions of the dopant concentration. Takeda [18] further detected Eu^{2+} on the A-site, using EPR at four different temperatures, the highest being 426 K, the Ba/Ti ratio was not specified.

High temperature conductivity vs oxygen partial pressure measurements is a very powerful tool for investigating doping effects. First to study intentionally-doped $BaTiO_3$ using this method were Daniels and Härdtl [19]. They have shown that La occupies the A-site in Ti-rich (and overall B-rich) samples. While we do not fully agree with the defect model proposed by Daniels and Härdtl, their experimental results clearly demonstrate the donoric behavior of the La. Takada et al. [20, 21] reported that Y and Er can occupy either A or B site depending on Ba-stoichiometry. This investigation included a series of conductivity vs oxygen partial pressure measurements on the following rare-earth dopants in both Ba- and Ti-rich compositions: Yb, Er, Dy, Sm and Nd. Despite one discrepancy in the relative behavior of Dy and Sm in Ba-rich compositions, they were able to show a gradual change from acceptoric behavior of the Yb through amphoteric behavior of the Er to donoric behavior of Nd.

Xue et al. [22] measured the room temperature conductivity of $BaTiO_3$ samples doped with all the lathanide series (except the radioactive Pm) as well as Sc, Y, Bi, Al, Ga and In. This was done with different A/B ratios, for air-fired samples. Their conclusion was that Y^{3+} and Er^{3+} are amphoteric while all smaller ions are acceptors (B-site) and larger ions are donors (A-site). Xue et al. did not observed the gradual change reported by Takada et al. [20] It is important to remember that this probe, namely, room temperature conductivity, is only sensitive to the overall frozen ionic charge, including vacancies of all kinds. This ionic charge is compensated in room temperature by electronic charge, which gives rise to orders of magnitude differences in conductivity according to its type: electrons or holes [23].

Makovec et al. [24] investigate the incorporation of high concentration of Ce into the lattice of $BaTiO_3$ by means of microanalysis of the phases formed. They concluded that Ce is incorporated into the lattice either as Ce^{4+} on the B-site or as Ce^{3+} on the A-site. The partitioning was found to depend primarily on the Ba/Ti ratio and slightly on the oxygen partial pressure and temperature during the sintering. The same group, using the same method found [25] that La is incorporated as 3+ into the A-site with Ti vacancies as the main compensating defects for concentrations of $\sim$1 mol%.

Zhi et al. [26] studied the incorporation of Y into $BaTiO_3$ using microanalysis and XRD on samples with different concentrations and nominal compositions. They found that Y is amphoteric, with higher solid solubility on the A-site. We would like to comment here that higher solubility limit in one site does not necessarily imply preferential occupancy on this site. It may rather be a result of the differences in the relevant chemical potentials of the second solid phases that are precipitate when the solubility limits are reached [27].

5. Structural Characterization

The main tool used in order to investigate site occupancy is powder XRD measurements, with error analysis using maximum likelihood estimation method [28]. As all the trivalent rare earth (RE) ions are larger than Ti^{4+} and smaller than Ba^{2+}, we assume that the lattice expands with RE on the B-site and shrinks with RE on the A-site. Several authors reported lattice expansion in perovskite chromites [29, 30] and titanates [31] as a result of reduction. Therefore we should also expect lattice expansion as a result of more electrons (due to reduction of Ti) and/or less metal vacancies.

In addition, some of the samples were also examined using electron paramagnetic resonance (EPR) spectroscopy. As this paper intends to present the full picture of our current understanding of the rare-earths in $BaTiO_3$, we will discuss here the results only. This will be given first for the more stable 3+ rare-earths and

then for multiple valence ions. The experimental details of the XRD measurements and sample preparation [9] and a full report on the EPR measurements [32] are described elsewhere.

5.1. *Stable Trivalent REs*

The results of the XRD measurements on stable trivalent dopants are summarized in Table 1 and Figs. 2 and 3. Using the maximum likelihood estimation method [28], we were able to accurately define the error bars in the tetragonal lattice parameters. The ionic radii are taken from CRC[6] for CN = 6.

We identified three regimes in Fig. 2, which are summarized below:

1. For ionic radii, $r \lesssim 0.87$ Å (Lu), the dopants occupy the B-site. The compensation is mainly via oxygen vacancies. For Ti rich samples, we expect more Ba vacancies and hence slightly smaller volumes.
2. For ionic radii, 0.87 Å $\lesssim r \lesssim$ 0.94 Å (Er, Y, Ho, Dy, Gd), the dopants capable of choosing their site during the firing according to the Ba/Ti ratio. We call them amphoteric dopants, since they are either acceptors or donors, according to their site. The manifestation of this in Fig. 2 is the fact that the volumes of Ba-rich samples with these dopants are larger than of Ti-rich samples. This follows from Eq. (4) and Vegard's law (see for instance p.131 in Kingery et al. [33]).
3. For ionic radii, 0.94 Å $\lesssim r$ (Nd, La), the dopants occupy the A-site. The main compensation mechanisms are Ba/Ti (or A/B) dependent [34]. For Ba/Ti = 0.99 we have A/B $\sim$ (Ba + RE)/Ti $\sim$ 1 and the compensation mechanism is mainly by electrons (and metal vacancies of both type) [34]. In this case the lattice expands (or less shrinks) with the dopant's ionic radius. For Ba/Ti = 1.01 we have A/B > 1 (although not A/B = 1.02, since a second Ba-rich phase is present) and a significant part of the compensation mechanism is by titanium vacancies [35]. The titanium vacancies, and maybe also differences in solubility, are responsible for the further shrinkage of the lattice.

Table 1. Unit cell volume at room temperature of $BaTiO_3$ doped with 1% various cations, as measured by XRD.

Dopant	Ionic radius/Å	Lattice volume/Å^3 Ba-rich (Ba/Ti = 1.01)	Lattice volume/Å^3 Ti-rich (Ba/Ti = 0.99)
Lu	0.861	64.527(17)	64.516(11)
Yb	0.868	64.5180(97)	64.4899(89)
Er	0.89	64.519(14)	64.453(14)
Y	0.9	64.469(13)	64.370(10)
Ho	0.901	64.472(15)	64.363(10)
Dy	0.912	64.444(16)	64.382(13)
Gd	0.938	64.368(17)	64.332(16)
Sm	0.958	64.321(17)	64.326(15)
Nd	0.983	64.298(20)	64.329(14)
La	1.045	64.311(15)	64.3842(99)

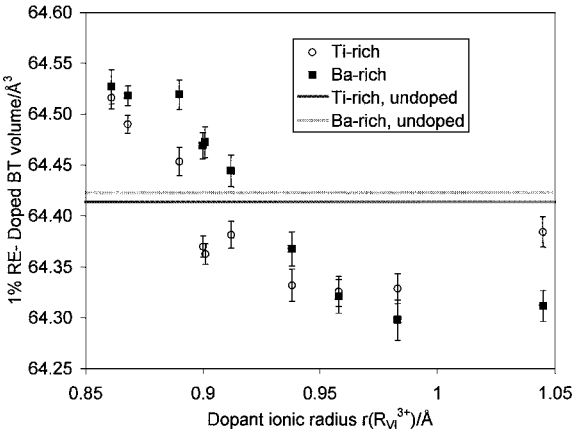

Fig. 2. Unit cell volume at room temperature of (left to right) Lu, Yb, Er, Y, Ho, Dy, Gd, Sm, Nd and La doped $BaTiO_3$ vs the octahedral ionic radius of the dopant.

Verification of these results was carried out with EPR measurements on selected samples. Specifically those containing dopants which are sensitive to the EPR

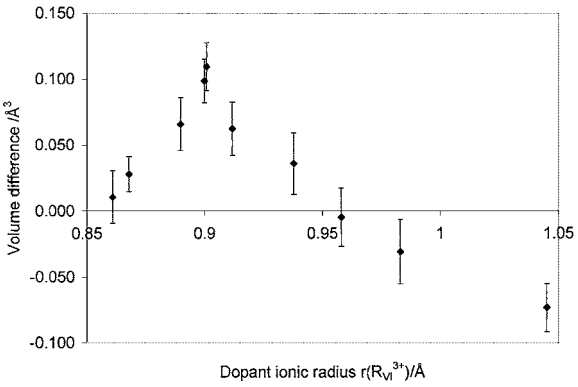

Fig. 3. The difference in unit cell volumes of Ba-rich and Ti-rich (Ba/Ti = 1.01 and 0.99 respectively) chemistries of doped $BaTiO_3$ vs the octahedral ionic radius of the dopant.

technique, i.e., dopants with an odd number of electrons, namely, Er^{3+}, Dy^{3+}, Gd^{3+}, and Nd^{3+}. Frequently the analysis of the EPR results is difficult due to possible contributions from impurities, multiple ion valences and defect interactions. However preliminary analysis shows a general agreement with the above mentioned XRD results. Consistent with earlier EPR results [14], Gd is found to be amphoteric for air-fired samples, and the degree of site occupancy is sensitive to the Ba/Ti ratio. This is inferred through the relative signal strength for the various samples in the EPR spectrum. Dy also demonstrates amphoteric behavior with a signal typical of B-site occupancy by Dy^{3+}, while showing none from the A-site. In Ba-rich samples, this signal is about three times as large as in Ti-rich samples. No signal typical of Dy^{3+} in the A-site is observed. A possible explanation to this is that Dy is forced to be 2+ on the A-site at low temperatures (the EPR measurement was done at 10 K). This is in accordance with the observation made by XRD in room temperature, where the B-rich sample containing Dy appears to be larger than expected, compared to the other sequence, see Fig. 2.

5.2. *Multiple Valence Ions*

Further measurements were performed on less stable dopants. The additional dopants measured with XRD were Yb, Tm, Eu and Sm that are known to exist as both 3+ and 2+, and Tb (Ba-rich only), Pr and Ce that are known to exist as both 3+ and 4+. These results are summarized in Fig. 4. All these samples were sintered in reducing atmosphere at $P(O_2) \sim 10^{-10}$ atm, and at temperatures $T \sim 1400^{\circ}$C.

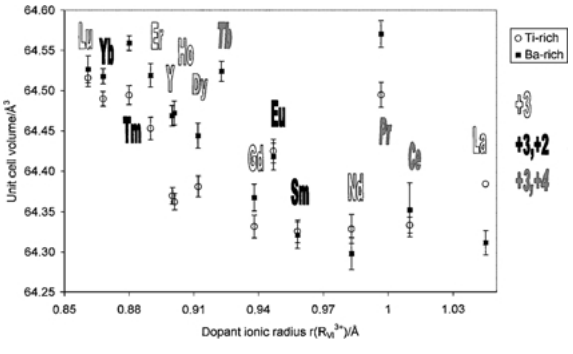

Fig. 4. Unit cell volume of Ba-rich and Ti-rich (Ba/Ti = 1.01 and 0.99 respectively) chemistries of doped $BaTiO_3$ vs the octahedral ionic radius of the dopant, including multiple valence dopants.

Sm, and Yb cations behave similar to the stable 3+ cations. The Sm incorporates as 3+ mainly into the A-site regardless the A/B ratio, and remains as 3+ ion on cooling even to room temperature. However, EPR suggests that Sm might be 2+ at 10 K. The Yb mostly occupies the B-site as a 3+, however from the XRD we can infer that a small degree of amphoteric behavior exists with $Yb^{\bullet}_{Ba}$ being more prevalent with Ti rich chemistries. Similar amphoteric behavior is observed for Tm, the offsets in the unit cell volume relative to Lu, Yb and Ho are believed to be associated with valence changes at low temperatures.

Eu on the other hand creates a relatively larger average cell volume, as compared to its neighbors Gd, Sm and Nd. This suggests that Eu in room temperature is mainly a 2+ ion on the A-site. It is not possible to infer from this data to the valence at which Eu is incorporated during the sintering process, i.e., $Eu^{\bullet}_{Ba}$ or $Eu^{\times}_{Ba}$.

Using EPR, Eu^{2+} was observed to be A-site in both Ba- and Ti-rich samples. Also, Yb was observed to be on the B-site, while no signal typical of Yb^{3+} on an A-site was observed. Combining this with the XRD measurements suggests that Yb on the A-site is 2+ at 10 K.

The ions which are capable of existing as 4+, namely Tb, Pr and Ce show even more interesting behavior in relation to their lattice relaxations in $BaTiO_3$. As explained in section 3, it is expected that during the sintering process it would be easier to get valence of 4+. Therefore, we anticipate a stronger tendency to occupy the B-site, due to both coulombic and strain interactions. Later, on cooling, these ions may act as electron traps on the B-site and therefore become larger, often refer to as a polaron distortion [36]. This phenomenon would be more expected with the aid of Ba-rich chemistry. In Fig. 4, the variation in the lattice volumes for Tb, Pr and Ce dopants relative to the other rare-earth ions can be readily accounted for from the above considerations. The results can be interpreted in the following manner: Tb in Ba-rich case is incorporated into the B-site as a 4+ ion during the sintering and on cooling to room temperature traps a single electron and becomes a large 3+ ion. Pr has a partitioning during the incorporation between the A and B-sites, with 4+ on the B-site. Again, it becomes a 3+ on cooling. The partitioning of site occupancy is influenced by the Ba/Ti ratio. Ce, being larger than Pr, tends more to the A-site. In room temperature it looks like a 3+ A-site ion for the Ti-rich case. In the

Ba-rich case it is larger, probably due to some B-site occupancy, with either 3+ or 4+ valence. According to Makovec et al. [24] it is 4+ on the B-site in this case.

5.3. *Influence of the Firing Atmosphere*

The oxygen partial pressure during the firing may influence the site occupancy and the valence of the dopant. As explained above, these two phenomena are interrelated. In this section we will discuss how this happens. It is important to remember that site occupancy and valence are more influenced by the nature of the dopant and by the A/B ratio. The oxygen partial pressure is only a secondary effect.

The site occupancy is controlled by the size of the ion, its valence, the A/B ratio (or the activity of titania in the system) and by the oxygen vacancy concentration (Eq. (4)). This, in principle, is $P(O_2)$ dependent. The most simple case is when two solid phases coexist in equilibrium below the solubility limit of the dopant. According to Gibbs' phase rule, the number of degrees of freedom is $f = c - p + 2$ where c is the number of chemical components and p is the number of phases. The number of chemical components is 3 (4 for doped systems) and for two solid phases in equilibrium the number of phases is 3 (including a gas phase). Therefore the number of degrees of freedom is $f = 2$ for undoped and $f = 3$ for doped systems. Those degrees of freedom can be chosen as the temperature and the oxygen partial pressure for undoped BT. For doped BT, the second solid phase is usually a sink for one of the cations (R_2O_3 above the solubility limit of the dopant, Ba_2TiO_4 for Ba rich, $Ba_6Ti_{17}O_{40}$ for Ti rich, to name the simplest examples). The third degree of freedom below the solubility limit of the dopant can be chosen as the concentration of the dopant, either in the whole system or in the BT. The activity of, for instance, the titania in the BT in this case, is a function of the above mentioned degrees of freedom and cannot be arbitrarily chosen (as in the case of a single solid phase, where it can be the additional degree of freedom). In addition, we assume that when the second solid phase serves as a sink for either Ba or Ti ions, the activity of titania (or BaO) is nearly a constant with respect to the oxygen partial pressure and the concentration of the dopant, i.e., it is to a first approximation a function of the temperature only. Under this approximation, it follows from Eq. (4) that the site occupancy ratio is proportional to the oxygen vacancy concentration [37]. The oxygen vacancy concentration is a weak function of the oxygen partial pressure, typically [37]

$$-\frac{1}{6} \lesssim \frac{\mathrm{d}(\log[V_{\mathrm{O}}^{\bullet\bullet}])}{\mathrm{d}(\log P(O_2))} < 0 \tag{6}$$

A summary of the influence of $P(O_2)$ on the site occupancy, as measured by lattice volumes for a variety of amphoteric dopants is given in Table 2. Although the uncertainties in the differences of the unit cell volumes are relatively large, the trend is clear: air fired samples have larger volumes than reduced fired samples. This is because air fired samples have less oxygen vacancies. This drives the site occupancy ratio towards more B-site occupancy, according to Eq. (4). Note that the previous works that reported lattice expansion due to reduction were done on samples with non-amphoteric dopants or on nominally undoped samples [29–31].

Table 2. The influence of the oxygen partial pressure on the site occupancy (this work): unit cell volumes in Å of samples fired in reducing atmosphere ($P(O_2) \sim 10^{-10}$ atm.) compared to samples fired in air.

	Dopant	Reducing	Air	Difference [Å^3]
Ba-rich	Yb	64.5180(97)	64.529(14)	0.011(17)
	Er	64.519(14)	64.548(12)	0.029(18)
	Y	64.469(13)	64.471(10)	0.002(16)
	Ho	64.472(15)	64.492(11)	0.020(19)
	Dy	64.444(16)	64.472(11)	0.028(19)
	Sm	64.321(17)	64.343(31)	0.022(35)
Ti-rich	Er	64.453(14)	64.5114(98)	0.058(17)
	Y	64.370(10)	64.428(14)	0.058(17)
	Ho	64.363(10)	64.417(16)	0.054(19)
	Dy	64.382(13)	64.416(16)	0.034(21)
	Sm	64.326(15)	64.334(24)	0.008(28)

In addition, regarding the valence of the dopant, one has to consider the reaction

$$R_M^Z + e' \Leftrightarrow R_M^{Z-1} \tag{7}$$

and its corresponding mass action relation

$$[R_M^Z]n = K(T)[R_M^{Z-1}] \tag{8}$$

The concentration of free electrons for a given temperature is also a function of the oxygen partial pressure, typically [37]

$$-\frac{1}{4} < \frac{\mathrm{d}(\log n)}{\mathrm{d}(\log \mathrm{P(O_2)})} \lesssim -\frac{1}{6} \tag{9}$$

We expect, therefore, that the concentration of lower valence states will be higher at lower oxygen partial pressure, for a given temperature. Further, for the special case where the partition is between a $R^{\bullet}_{\mathrm{Ba}}$ and $R^{\times}_{\mathrm{Ti}}$ such as with Ce, the site occupancy ratio is controlled both by Eq. (4) and the hole concentration. This gives rise to a higher dependence of the site occupancy ratio on $\mathrm{P(O_2)}$.

6. Summary

The various issues discussed in the text are now summarized for each rare-earth dopant in $BaTiO_3$, also see Table 3. This is aimed to give a clear picture of our current understanding of the rare-earths in $BaTiO_3$.

6.1. Lanthanum

La is a stable donor on the A-site: $\mathrm{La}^{\bullet}_{\mathrm{Ba}}$. The compensation is done by electrons and metal vacancies, with a transition from mainly electron compensation to mainly metal vacancy compensation with increasing concentration of La [2]. Recently it was shown analytically, using doping factor considerations [38], that transition in compensation mechanism should be expected [34]. The solubility of La in $BaTiO_3$ is higher for A-rich chemistries, i.e., where the system is adjusted for Ti vacancy compensation.

6.2. Cerium

Ce is a multivalent ion which is most probably incorporated as both 4+ on the B-site: $\mathrm{Ce}^{\times}_{\mathrm{Ti}}$ and 3+ on the A-site: $\mathrm{Ce}^{\bullet}_{\mathrm{Ba}}$. This was first reported by Makovec et al. [24] and is also consistent with our XRD data. (However, our EPR results show no signal from Ce^{3+} at 10 K). The partition is influenced by the A/B ratio and somewhat also by the oxygen partial pressure. Lowering the oxygen partial pressure for a given Ba/Ti ratio should drive the incorporation towards the A-site (this prediction is yet to be checked experimentally).

Table 3. Summary of rare-earth cations in $BaTiO_3$.

	A-site radii [Å]	B-site radii [Å]	A-site valence[a]	B-site valence[a]	Main incorporation[b]
La	1.320	1.045	3+	N/A	A-site
Ce	1.290	0.87/1.010	3+	4+/3+	A-site 3+ and B-site 4+. The partition depends on $\mathrm{P(O_2)}$, T and A/B during the incorporation.
Pr	1.286	0.85/0.997	3+	4+/3+	A-site 3+ and B-site 4+
Nd	1.276	0.983	3+	3+	A-site
Sm	1.260/?	0.958/1.19	3+/2+	3+	A-site
Eu	1.252/?	0.947/1.17	3+(?)/2+	?	A-site
Gd	1.246	0.938	3+	3+	amphoteric, leans towards A-site
Tb	1.236	0.76/0.923	3+	4+/3+	B-site 4+
Dy	1.228/?	0.912/1.07	3+/2+	3+	amphoteric
Ho	1.221	0.901	3+	3+	amphoteric
Er	1.214/?	0.890	3+/2+	3+	amphoteric
Tm	1.207/?	0.880/1.03	3+/2+	3+	amphoteric, leans towards B-site
Yb	1.199/?	0.868/1.02	3+/2+	3+	B-site
Lu	1.194	0.861	N/A	3+	B-site

[a]Valence between the incorporation and room temperature.
[b]Other incorporation modes might be possible, see text.

6.3. Praseodymium

Pr is also a multivalent ion, slightly smaller than Ce. It is therefore behaves similar to Ce during the incorporation, with more tendency to occupy the B-site than Ce. On cooling to room temperature it becomes 3+ and therefore expands the lattice. The fact that the incorporation to the B-site is done isovalently has an important implication: the compensation of the lower temperature acceptor Pr'_{Ti} is done mainly by electronic charge. In addition, one may anticipate higher solubilities for isovalent substitutions [27].

6.4. Neodymium

Nd is a stable 3+ ion, which like La is going mainly to the A-site.

6.5. Samarium

Sm is known to be a 2+ as well as a 3+ ion. At high temperatures it is 3+ and behaves like La and Nd. The experimental data suggest that at room temperature it is also 3+. This is in accordance with the room temperature conductivity measurements of Rotenberg et al. [16]. The lack of signal in the EPR measurements suggest that it is 2+ at 10 K.

6.6. Europium

Eu is also known to be a 2+ as well as a 3+ ion. From room temperature XRD measurements it is clear that Eu is 2+ on the A-site. EPR measurements confirmed this for 10 K–294 K. It is not known at the moment if and at what temperature range it becomes a 3+ ion.

6.7. Gadolinium

Gd is an amphoteric ion with strong tendency towards the A-site [14]. EPR measurements confirm that most of the Gd^{3+} is at the A-site. Since for a given A/B ratio, lower oxygen partial pressure during the sintering drives amphoteric ions towards higher A-site occupancy [37], it is expected to be less amphoteric at low oxygen partial pressure. It is therefore probably not a good candidate to improve lifetime of base metal electrode MLCs, like other amphoteric dopants [39].

6.8. Terbium

Tb is a mixed 3+, 4+ ion. Being smaller than Pr, it is probably incorporated more on the B-site than Pr, however, the expansion of the lattice is less in Ba-rich Tb doped $BaTiO_3$ than in Ba-rich Pr doped $BaTiO_3$.

6.9. Dysprosium

Dy is an amphoteric dopant in $BaTiO_3$. Its solubility limit is higher on the A-site [40]. At lower temperatures some of the $Dy^{\bullet}_{Ba}$ become 2+, and therefore $Dy^{\times}_{Ba}$. At 10 K, as observed by EPR, probably all the Dy on the A-site is 2+. This may explain the "bump" in Ti-rich Dy doped $BaTiO_3$ seen in Fig. 2.

6.10. Holmium

Ho is the most amphoteric RE dopant in $BaTiO_3$, namely it is a very stable 3+ ion which is easily influenced by the local Ba/Ti ratio in terms of its site occupancy. Y is very close in size to Ho and is also amphoteric.

6.11. Erbium

Er is an amphoteric dopant [16] that show higher amphoteric behavior at lower oxygen partial pressure sintering, as confirmed by XRD measurements. EPR measurements at 10 K show significant lower signal of Er^{3+} in low oxygen partial pressure fired samples. This suggests that part of the Er is 2+ in those samples. This is also consistent with the XRD results of Fig. 4, where it appears that the lattice volume of the Er doped samples is relatively larger than expected. Further investigation of this issue is needed, since Er is generally considered as a stable 3+ ion.

6.12. Thulium

Tm^{3+} is relatively small and hence occupy mainly the B-site. Some degree of amphotericity is possible. Room temperature XRD suggests that there exists mixed valence, as generally accepted. At lower temperatures higher concentration of Tm^{2+} is expected.

6.13. Ytterbium

Yb^{3+} is also relatively small and hence occupy mainly the B-site. Some degree of amphotericity is possible. Room temperature XRD can be interpreted as it maintains its 3+ charge down to this range of temperatures. A signal from Yb^{3+} is also observed with EPR at 10 K. The fact that Yb goes to the B-site may enhance the stability of Yb^{3+} in $BaTiO_3$. EPR revealed that Yb was on the B-site and that the signal intensity was the same regardless of whether or not the sample was Ba- or Ti-rich. Furthermore, no signal was observed for Yb^{3+} on the A-site.

6.14. Lutetium

Lu is a stable 3+ ion. Being the smallest rare-earth ion it occupies only the B-site. (An even smaller stable 3+ ion suitable for B-site substitution is, of course, Sc).

Acknowledgments

We wish to thank the members of the Center for Dielectric Studies for their financial support. This work performed in part at Sandia National Laboratories. This part was supported by the US Department of Energy under Contract No. DE-AC04-94AL85000. We also wish to thank Dr. D. Fazuzou for many useful discussions.

References

1. A.J. Moulson and J.M. Herbert, *Electroceramics: Materials, Properties and Applications* (Chapman-Hall, London, 1990).
2. G.H. Jonker, *Solid State Elect.*, **7**, 895 (1964).
3. H. Kishi, N. Kohzu, J. Sugino, H. Oshato, Y. Iguchi, and T. Okuda, *J. Eur. Ceram. Soc.*, **19**, 1043 (1999).
4. R.S. Roth, *J. Res. Natl. Bur. Std.*, **58**, 75 (1957).
5. R.D. Shannon, *Inorganic Chem.*, **6**, 1474 (1967).
6. D.R. Lide, *CRC Handbook of Chemistry and Physics* (CRC Press, 2000), Ch. 4-121.
7. F.A. Kröger and H.J. Vink, *Solid State Physics*, **3**, 307 (1956).
8. R. Wernicke, *Philips Res. Repts.*, **31**, 526 (1976).
9. Y. Tsur, H. Hitomi, I. Scrymgeour, and C.A. Randall, *Jpn. J. Appl. Phys.*, **40**, 255 (2001).
10. R. Moos and K.H. Härdtl, *J. Am. Ceram. Soc.*, **78**, 2569 (1995).
11. Y.M. Chiang and T. Takagi, *J. Am. Ceram. Soc.*, **73**, 3278 (1990).
12. K. Sasaki and J. Maier, *J. Eur. Ceram. Soc.*, **19**, 741 (1999).
13. L. Rimai and G.A. deMars. *Phys. Rev.*, **127**, 702 (1962).
14. T. Takeda and A. Watanabe, *J. Phys. Soc. Jpn.*, **19**, 1742 (1964).
15. G. Goodman, *J. Am. Ceram. Soc.*, **46**, 48 (1963).
16. B.A. Rotenberg, Yu. L. Danilyuk, E.I. Gindin, and V.G. Prokhvatilov, *Soviet Phys.—Solid State*, **7**, 2465 (1966).
17. O. Saburi, *J. Phys. Soc. Japan*, **14**, 1159 (1959).
18. T. Takeda, *J. Phys. Soc. Jpn.*, **24**, 533 (1968).
19. J. Daniels and K.H. Härdtl, *Philips Res. Rep.*, **31**, 489 (1976).
20. K. Takada, E. Chang, and D.M. Smyth, *Advances in Ceramics*, **19**, 147 (1987). Multilayer Ceramic Devices, eds. J.B. Blum and W.R. Cannon. *Am. Ceram. Soc.*, Westerville, Ohio.
21. K. Takada, H. Ichimura, and D.M. Smyth, *Jpn. J. Appl. Phys.*, Suppl., **26**, 42 (1987).
22. L.A. Xue, Y. Chen, and R.J. Brook, *Mater. Sci. Eng.* **B1**, 193 (1988).
23. R. Waser. *J. Am. Ceram. Soc.*, **74**, 1934 (1991).
24. D. Makovec, Z. Samardzija, and D. Kolar, *Third Euro-Ceramics*, **1**, 961 (1993).
25. D. Makovec, Z. Samardzija, U. Delalut, and D. Kolar, *J. Am. Ceram. Soc.*, **78**, 2193 (1995).
26. J. Zhi, A. Chen, Y. Zhi, P.M. Vilarinho, and J.L. Baptista, *J. Am. Ceram. Soc.*, **82**, 1345 (1999).
27. Y. Tsur and I. Riess, *Z. Physik. Chem. (Munich)*, **207**, 181 (1998).
28. Y. Tsur and C.A. Randall, *J. Am. Ceram. Soc.*, **83**, 2062 (2000).
29. T.R. Armstrong, J.W. Stevenson, L.R. Pederson, and P.E. Raney, *J. Electrochem. Soc.*, **143**, 2919 (1996).
30. A. Atkinson and T.M.G.M. Ramos, *Solid State Ionics*, **129**, 259 (2000).
31. P.R. Slater, D.P. Fagg, and J.T.S. Irvine. *J. Mater. Chem.*, **7**, 2495 (1997).
32. T. Dunbar, Y. Tsur, and C.A. Randall, In preparation.
33. W.D. Kingery, H.K. Bowen, and D.R. Uhlmann, *Introduction to Ceramics* (Wiley, New York, 1976).
34. Y. Tsur and C.A. Randall, Charge-compensation in barium titanate, in *Proc. Int. Symp. Appl. Ferroelectrics* (IEEE, 2000).
35. H.M. Chan, M.P. Harmer, and D.M. Smyth. *J. Am. Ceram. Soc.*, **69**, 507 (1986).
36. D. Alder, in *Solid State Chemistry vol. 2*, edited by N.B. Hanning (Plenun, London, 1967).
37. Y. Tsur and C.A. Randall, in *High Temperature Corrosion and Materials Chemistry*, edited by P.Y. Hou, T. Marayama, M.J. McNallan, T. Narita, E.J. Opila, and D.A. Shores (Electrochemical Society, 2000), p 502.
38. Y. Tsur and I. Riess, *Phys. Rev.* B, **60**, 8138 (1999).
39. Y. Tsur and C.A. Randall, in *Fundamental Physics of Ferroelectrics*, edited by R.E. Cohen (AIP, New York, 2000), p 283.
40. W.-H. Lee, W.A. Groen, H. Schreinemacher, and D. Hennings. *J. Electroceram.*, **5**, 31 (2000).